



available at www.sciencedirect.com



www.elsevier.com/locate/yexcr



## Research Article

# Identification of a novel centrosomal protein Crp<sup>F46</sup> involved in cell cycle progression and mitosis

Yi Wei<sup>a,1</sup>, Enzhi Shen<sup>a,1</sup>, Na Zhao<sup>a</sup>, Qian Liu<sup>a</sup>, Jinling Fan<sup>a</sup>, Jan Marc<sup>b</sup>,  
Yongchao Wang<sup>a</sup>, Le Sun<sup>c</sup>, Qianjin Liang<sup>a,\*</sup>

<sup>a</sup>Key Laboratory of Cell Proliferation and Regulation Biology of Ministry of Education, College of Life Sciences, Beijing Normal University, Beijing 100875, PR China

<sup>b</sup>School of Biological Sciences, University of Sydney, Sydney 2006, Australia

<sup>c</sup>Welson Pharmaceuticals, Haidian, Beijing 100085, PR China

## ARTICLE INFORMATION

### Article Chronology:

Received 19 June 2007

Received in revised form

25 February 2008

Accepted 28 February 2008

### Keywords:

Antisense RNA

Cell cycle

Cell proliferation

Centrosome-related protein

Crp<sup>F46</sup>

Cytokinesis

Golgin-245

HeLa cells

Mitosis

## ABSTRACT

A novel centrosome-related protein Crp<sup>F46</sup> was detected using a serum F46 from a patient suffering from progressive systemic sclerosis. We identified the protein by immunoprecipitation and Western blotting followed by tandem mass spectrometry sequencing. The protein Crp<sup>F46</sup> has an apparent molecular mass of ~60 kDa, is highly homologous to a 527 amino acid sequence of the C-terminal portion of the protein Golgin-245, and appears to be a splice variant of Golgin-245. Immunofluorescence microscopy of synchronized HeLa cells labeled with an anti-Crp<sup>F46</sup> monoclonal antibody revealed that Crp<sup>F46</sup> localized exclusively to the centrosome during interphase, although it dispersed throughout the cytoplasm at the onset of mitosis. Domain analysis using Crp<sup>F46</sup> fragments in GFP-expression vectors transformed into HeLa cells revealed that centrosomal targeting is conferred by a C-terminal coiled-coil domain. Antisense Crp<sup>F46</sup> knockdown inhibited cell growth and proliferation and the cell cycle typically stalled at S phase. The knockdown also resulted in the formation of poly-centrosomal and multinucleate cells, which finally became apoptotic. These results suggest that Crp<sup>F46</sup> is a novel centrosome-related protein that associates with the centrosome in a cell cycle-dependent manner and is involved in the progression of the cell cycle and M phase mechanism.

© 2008 Published by Elsevier Inc.

## Introduction

The centrosome is a multifunctional organelle best known for its function as a major microtubule-organizing center in metazoan cells [1–3]. During interphase the centrosome nucleates a radial array of microtubules of uniform polarity, which extend to the cell periphery and drive the cellular distribution of cytoplasmic organelles. The centrosome normally replicates during the S phase, forming two daughter

centrosomes that migrate to the opposite poles of the cell where they direct the assembly of a bipolar mitotic spindle and play an important role in the organization and orchestration of mitosis. At cytokinesis, each daughter cell inherits one centrosome. Thus, at any time during interphase, a normal cell contains either one centrosome (G1/G0 phase) or two duplicated centrosomes (late S or G2 phase).

The centrosome consists of a pair of cylindrical centrioles surrounded by a matrix of protein aggregates (pericentriolar

\* Corresponding author. Fax: +86 10 58807720.

E-mail address: Lqj@bnu.edu.cn (Q. Liang).

<sup>1</sup> These authors contributed equally to this work.

material, PCM). The two centrioles act as basal bodies for the assembly of cilia and flagella [4]. The PCM harbors hundreds of proteins that perform diverse functions, including the integration of signaling pathways and regulation of cellular processes in addition to its well established role as the primary microtubule-organizing center [3,5,6]. Among the characterized centrosomal proteins are  $\gamma$ -tubulin complexes and other cytoskeletal regulators including microtubule-associated proteins, motor proteins, cell-cycle regulators, checkpoint proteins, kinases and phosphatases, calcium-binding proteins, signaling proteins, structural/scaffold proteins, ubiquitination and protein degradation, and many other proteins whose function remains to be determined [7,8].

The replication of centrosomes is strictly controlled by a molecular mechanism that "licenses" centrosome duplication and "blocks" re-duplication [9]. When a cell loses control of centrosome duplication, centrosome amplification occurs, leading to the formation of aberrant mitotic spindles, multipolarity, and chromosome missegregation during mitosis [10–13]. Aberrant amplification of centrosomes can be induced by mutations in various cell-cycle regulatory proteins [14–17], loss of tumor suppressor proteins and other pathological changes [18–21]. The exact molecular mechanism controlling centrosome replication is unclear.

Antibodies present in the sera of patients with autoimmune diseases, such as systemic lupus erythematosus and scleroderma polymyositis, have become a valuable and important resource for identifying new cellular constituents [22–24]. These include centromere (kinetochore)-related proteins [25,26], SCL-70/topoisomerase I [27], RNA polymerase I [28] and proteins associated with uridine-rich small nuclear RNAs (U RNAs) [29]. Advances in proteomics have dramatically accelerated the process of identifying new proteins. Because the sequencing of some proteins has been complicated by the presence of blocked amino termini, tandem mass spectrometry (MS/MS) has become a powerful tool of direct peptide sequencing for identification and comparison of related proteins [30–33]. In the present study, we used autoimmune serum F46 from a patient suffering from progressive systemic sclerosis to immunoprecipitate the target protein from HeLa cell lysate. MS/MS sequencing [34,35] and deletion fragment analysis showed that it is a novel protein with predicted molecular mass of 62.6 kDa, formed as a splice variant of the C-terminal portion of Golgin-245. Immunofluorescence labeling of synchronized HeLa cells revealed that the protein localizes exclusively to the centrosome during interphase but disappears at the onset of mitosis. We named the protein "centrosome-related protein F46" (Crp<sup>F46</sup>). Depletion of Crp<sup>F46</sup> by antisense RNA caused the formation of poly-centrosomal and multinucleate cells, inhibition of cell proliferation, and arrest at the S phase. These results suggest that Crp<sup>F46</sup> may be a critical factor in cell-cycle progression and M phase regulation.

## Materials and methods

### Cell culture, reagents, and antibodies

HeLa cells were cultured in Dulbecco's modified Eagle's medium (DMEM) (Invitrogen, USA) containing 10% (v/v) fetal

calf serum (FCS) (Sanli Biotechnology, Wuhan, China) at 37 °C in the presence of 5% CO<sub>2</sub>. Among the reagents used in this study were the reagent G418 (Merck, USA), rabbit anti-goat and goat anti-mouse IgG conjugates with FITC, and TRITC-conjugated goat anti-rabbit IgG (both from Vector Laboratories, Peterborough, UK). The polyclonal antibody against  $\gamma$ -tubulin was from Santa Cruz Biotechnology, USA, and an anti-PLK1 antibody from Cell Signaling Technology, USA. Oligonucleotides were synthesized by Sangon (Shanghai Sangon Biotechnology, Shanghai, China). Autoantiserum F46 was from a patient with progressive systemic sclerosis (Peking Union Medical Hospital, China).

### Immunoprecipitation of Crp<sup>F46</sup> protein and sequencing

Total protein extracts of HeLa cell were incubated with F46 serum (1:100 dilution) at 4 °C overnight and then incubated with Protein A plus-Sepharose (Dingguo Biotechnology, Beijing, China). The beads were washed three times with phosphate-buffered saline (PBS) containing 0.1% Triton X-100, and bound proteins were eluted by heating at 100 °C for 5 min. The eluted proteins were separated by SDS-PAGE using 12% gels. The polypeptide band of interest was excised and digested *in situ* with trypsin, and the resulting peptides were submitted for protein sequencing by tandem mass spectrometry (MS/MS) [36]. The protein sequence of Crp<sup>F46</sup> was used to search for homologous proteins in the NCBI/EMBL protein database using BLASTP.

### Cloning of Crp<sup>F46</sup> cDNA

The cDNAs were synthesized by RT-PCR using HeLa total RNA prepared by extraction with Trizol reagent (Invitrogen, USA). The RT-PCR was conducted in single (one-step) reactions by using M-MLV retro-transcriptional enzyme (Promega, USA). Primers for gradient PCR were synthesized according to the Crp<sup>F46</sup> peptide sequence: 5'-GGAAAGTTCACAGTCAGAAACA-3' and 5'-AGATCGGAGCCATGACATCA-3'. The PCR product was inserted into TA cloning vector (TaKaRa, Japan) to construct a recombinant plasmid pMD18-T-Crp<sup>F46</sup>.

### Co-immunoprecipitation of Crp<sup>F46</sup>, $\gamma$ -tubulin, and Plk1

Cells were washed in PBS and lysed in HEPES buffer (50 mM HEPES, pH 7.5, 150 mM NaCl, 1 mM MgCl<sub>2</sub>, 1 mM EGTA) containing protease inhibitors and 0.5% Triton X-100 for 5 min on ice. After centrifugation for 10 min at 16,000 g at 4 °C, cleared lysates were obtained. For immunoprecipitation, extracts were incubated with antibodies against Crp<sup>F46</sup>,  $\gamma$ -tubulin, PLK1, or Golgin-245 overnight at 4 °C. Subsequently, Protein A plus-Sepharose was added and the mixture incubated for 3–4 h at 4 °C. After centrifuging for 30 s at 4 °C, the pellets were washed five times with 500  $\mu$ l of cell-lysis buffer while keeping on ice. Washed pellets of protein complexes were resuspended in 20  $\mu$ l SDS sample buffer, vortexed, boiled, centrifuged for 30 s, and analyzed by SDS-PAGE and Western blotting.

### Preparation of monoclonal antibody against Crp<sup>F46</sup>

The coding sequence of Crp<sup>F46</sup> was amplified by PCR using the pMD18-T-Crp<sup>F46</sup> plasmid as a template. The primers were 175

176 5'-ACGGCGATCCATGGAAAGTTCACAGTCAG-3' and 5'-CCG-  
 177 GAATTC<sup>T</sup>CAAGATGAAGATCGG-3'. The PCR product was  
 178 then cleaved with BamHI/EcoRI enzymes and inserted into  
 179 corresponding restriction sites in pGEX-2Z (constructed by  
 180 pGEX-2T at the multiple-cloning site). Recombinant protein  
 181 was expressed in BL21(DE3) cells induced with 0.5 mM  
 182 isopropyl-1-thio-β-D-galactopyranoside (IPTG), and the pur-  
 183 ified protein was submitted for the preparation of monoclonal  
 184 antibody (Welson Biotechnology, Beijing, China).

#### 185 Construction of recombinant pEGFP expression vectors with 186 Crp<sup>F46</sup> fragments

187 Deletion fragments of Crp<sup>F46</sup> sequence corresponding to amino  
 188 acid residues 1–241, 127–426, and 323–530, each containing one of  
 189 the three coiled-coil domains, were prepared by PCR amplifica-  
 190 tion of the Crp<sup>F46</sup> cDNA using the following pairs of primer  
 191 sequences: 5'-GGGAAGCTTGAAAGTTCACAGTCAGAAAC-3' and  
 192 5'-ACGGCGATCCTCCAAGCAGCAG-3'; 5'-CCGAAGCTTG-  
 193 AAAGTTCACAGTC-3' and 5'-CGCGGATCCGGCTAATTTAA-3';  
 194 5'-CCCAAGCTTAAGCAAACTTGG-3' and 5'-CGCGGAT-  
 195 CCTTGCTCTTTC-3'; 5'-CCCAAGCTTCAGGAGGTGGAG-3' and  
 196 5'-CGCGGATCCTCAAGATGAAGAT-3'.

197 The PCR products were cleaved with HindIII/BamHI  
 198 enzymes and inserted into corresponding restriction sites in  
 199 the expression vector pEGFP-C3 (gift from Dr. Wanjie Li,  
 200 Beijing Normal University, China). The recombinant vectors  
 201 were transiently transfected into HeLa cells by using high-  
 202 efficiency transfection reagent Vigofect according to the  
 203 manufacturer's instruction (Vigorse, Beijing, China). Forty  
 204 eight hours after transfection, cells expressing GFP fusion  
 205 protein were counter-stained with γ-tubulin antibody (diluted  
 206 1:30) followed by and TRITC-conjugated goat anti-rabbit IgG  
 207 antibody (diluted 1:50), and examined with Olympus laser-  
 208 scanning confocal microscope (Olympus Fluoview FV300,  
 209 Japan).

#### 210 Construction of antisense Crp<sup>F46</sup> RNA and antisense golgin- 211 245 RNA expression vectors and stable transformation of 212 HeLa cells

213 A pXJ41 antisense-Crp<sup>F46</sup> vector was constructed by PCR  
 214 amplification of the entire coding sequence of Crp<sup>F46</sup> using  
 215 pMD18-T-Crp<sup>F46</sup> as a template. The PCR product was ligated in  
 216 reverse orientation into HindIII/EcoRI sites of pXJ41-neo vector  
 217 (gift from Dr. Xiaoyu Zhu, Beijing Normal University, China),  
 218 and the fidelity of ligation was confirmed by sequencing using  
 219 the primers 5'-GGGAAGCTTGAAAGTTCACAGTCAG-3' and  
 220 5'-CCGGAATTCGTAGATGAAGATCGG-3'.

221 A pCDNA3.1+ antisense golgin-245 vector was constructed by  
 222 PCR amplification of the N-terminus sequence of golgin-245,  
 223 using pMD18-T-N-terminus of Golgin-245 as a template.  
 224 Primers for gradient PCR were synthesized according to the  
 225 320–1627 bp region of golgin-245: 5'-ATGGCACAGGCTAACT-  
 226 CAG-3' and 5'-TTTATTGGACCAGTCATCTACC-3'. The PCR pro-  
 227 duct was ligated in reverse orientation into BamHI/HindIII  
 228 sites of pCDNA3.1+ vector (gift from Dr. Wanjie Li, Beijing  
 229 Normal University, China), and the fidelity of ligation was  
 230 confirmed by sequencing using the primers 5'-CGGGATCCGGC-  
 231 TAACTCAGC-3' and 5'-CCCAAGCTTGGACCAGTCATCTA-3'.

The recombinant DNA construct pXJ41 antisense-Crp<sup>F46</sup> 232  
 and an empty vector pXJ41-neo, and similarly the pCDNA3.1+ 233  
 antisense golgin-245 vector and the empty vector, were 234  
 transfected into HeLa cells by using the transfection reagent 235  
 Vigofect. Expression of the antisense molecule is driven by the 236  
 cytomegalovirus promoter of the vector transformed cells 237  
 were selected by culturing in the presence of G418 reagent 238  
 (60 ng/ml) for 14 days, and transgenic cell lines that were 239  
 stably silencing Crp<sup>F46</sup> were established. These cells were then 240  
 either fixed for immunostaining or processed for protein 241  
 extraction and immunoblot analysis. 242

#### Cell growth curves 243

Stably transformed antisense RNA cells and control cells were 244  
 seeded in 96-well plates at a density of 1 × 10<sup>4</sup> cells per well in 245  
 DMEM containing 10% FCS, and grown at 37 °C in the presence 246  
 of 5% CO<sub>2</sub>. Three wells of cells from each cell line were 247  
 harvested everyday for up to 7 days. A liter stock solution of 248  
 5 mg/ml MTT reagent (Sigma, USA) in PBS was then diluted 249  
 1:10 in DMEM without FCS, and 100 μl of this solution were 250  
 added to each well after aspirating the original media. 251  
 Following 4 h incubation at 37 °C, the cells were lysed with 252  
 100 μl DMSO and incubated for a further 10 min at 37 °C with 253  
 gentle shaking. Absorbance at 540 nm was determined using a 254  
 microplate analyzer (BIO-RAD Laboratories, USA). 255

#### Cell synchronization 256

HeLa cells in exponential growth phase were cultured in 257  
 DMEM with 10% FCS and 2 mM TdR for 16 h. The cells were 258  
 then washed with fresh DMEM containing 10% FCS, and 259  
 allowed to grow for an additional 9 h. At this time, 2 mM TdR 260  
 was again added, and the cells were incubated for another 261  
 16 h. The cells were then washed again with a fresh medium, 262  
 and allowed to grow for defined intervals as follows: 0 h in 263  
 order to collect cells arrested in G1/S phase, 5 h for arrest in 264  
 S phase, and 9 h for arrest in G2 phase. For M phase, the cells 265  
 were cultured for 15 h in DMEM containing 10% FCS and 266  
 200 ng/ml nocodazole (Sigma, USA). 267

#### Flow cytometry 268

Cells were trypsinized, washed three times with cold PBS, and 269  
 then fixed with 70% ethanol at 4 °C overnight. Following 270  
 digestion with RNase for 30 min at 37 °C, propidium iodide (PI) 271  
 (Sigma, USA) was added to a final concentration of 65 μg/ml. 272  
 Flow cytometric analysis was performed on a FACS Calibur (BD 273  
 Biosciences, USA). 274

#### Western blot analysis 275

Total protein extracts of HeLa cells or E. coli cells expressing 276  
 GST-Crp<sup>F46</sup> fusion protein were loaded onto 12% gels, sepa- 277  
 rated by SDS-PAGE, and transferred onto a nitrocellulose 278  
 membrane for 2 h at 200 mA. The membrane with transferred 279  
 polypeptides was immersed in 5% skim milk in PBST (PBS 280  
 containing 0.1% Tween 20) at room temperature for 1 h. After 281  
 two rinses with PBST, the proteins were probed with F46 282  
 serum (1:2000) or anti-Crp<sup>F46</sup> monoclonal antibody (1:500) at 283

Q1

284 room temperature for 1 h. The membrane was then incubated  
 285 with alkaline phosphatase-conjugated horse anti-mouse IgG  
 286 (1:1000) and the immunoreactions detected with nitro-blue  
 287 tetrazolium/5-bromo-4-chloro-3-indolyl phosphate (NBT/  
 288 BCIP) (Promega, USA).

#### 289 Immunostaining of cells

290 HeLa cells grown on coverslips were washed with PBS and  
 291 fixed either with methanol at  $-20^{\circ}\text{C}$  for 8 min or with 3.7%  
 292 paraformaldehyde at room temperature for 10 min, followed  
 293 by permeabilization with 0.25% Triton X-100 at room tem-  
 294 perature for 10 min. After washing three times with PBS and  
 295 blocking for 30 min with 5% skim milk in PBS, the coverslips  
 296 with cells were incubated with primary antibodies for 1 h at  
 297 room temperature. The primary antibodies were as follows:  
 298 a mouse anti-Crp<sup>F46</sup> monoclonal antibody (1:100), rabbit anti-  
 299  $\gamma$ -tubulin polyclonal antibody (1:100) (Santa Cruz Biotechnol-  
 300 ogy, USA), and goat anti- $\alpha$ -tubulin polyclonal antibody (1:100)  
 301 (Santa Cruz Biotechnology, USA). The cells were then washed  
 302 three times for 10 min each in PBST, and incubated for 1 h at  
 303  $37^{\circ}\text{C}$  with the secondary antibodies. The secondary antibodies  
 304 used were FITC-conjugated goat anti-mouse IgG (1:100),  
 305 TRITC-conjugated goat anti-rabbit IgG (1:100), or FITC homo-  
 306 anti-goat IgG (1:100) (all three antibodies were from Vector  
 307 Laboratories, USA). The cells were then washed three times  
 308 with PBST, counter-stained with propidium iodide (PI) or  
 309 diamidino-2-phenylindole (DAPI) (Sigma, USA), and mounted  
 310 in antifade mounting solution. The preparations were  
 311 observed with Olympus confocal laser-scanning microscope  
 312 (Olympus Fluoview FV300, Japan).

## 314 Results

### 315 Identification and characterization of centrosome-related 316 protein Crp<sup>F46</sup>

317 In a preliminary experiment, we used a serum F46 from a  
 318 patient suffering from progressive systemic sclerosis to  
 319 immunolabel HeLa cells. The immunoreaction showed that  
 320 the target protein localized as one or two dots adjacent to the  
 321 nucleus in interphase cells. This localization was similar to  
 322 the images shown in the detailed immunofluorescence  
 323 characterization below. In order to determine the size of the  
 324 target protein, total proteins were extracted from HeLa cells  
 325 separated by SDS-PAGE, transferred onto nitrocellulose mem-  
 326 brane, and probed with the F46 serum. The immunoreaction  
 327 revealed a distinct band of apparent molecular mass ( $M_r$ )  
 328 of  $\sim 60$  kDa (Fig. 1). Thus the F46 serum recognizes a unique  
 329 protein that appears to localize to the centrosome.

330 The identity of the protein was determined by immunopre-  
 331 cipitation with the serum F46 followed by SDS-PAGE, isolation  
 332 of the polypeptide band, digestion with trypsin, and protein  
 333 sequencing by tandem mass spectrometry (MS/MS) (Supple-  
 334 ment 1). Analysis of the peptide sequences using BLASTp  
 335 showed that the polypeptide is identical to a 527 amino acids  
 336 sequence of the C-terminal portion of Golgin-245 (Fig. 2). The  
 337 theoretical pI of Crp<sup>F46</sup> is 5.82, with predicted molecular mass of  
 338 62.6 kDa (predicted by PeptideMass) [37]. We named the protein

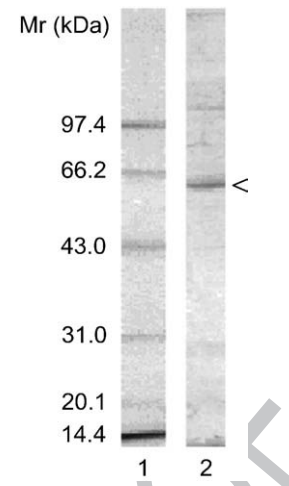


**Fig. 1 - Western blot analysis of HeLa proteins using F46 serum. Total HeLa cell proteins were separated by SDS-PAGE, transferred onto nitrocellulose membrane, and probed with F46 serum. The immunoblot (lane 2) reveals a distinct band of  $M_r \sim 60$  kDa (arrow).**

“centrosome-related protein F46” (Crp<sup>F46</sup>). Analysis of the 339  
 Crp<sup>F46</sup> sequence using SMART (simple modular architecture 340  
 research tool; [smart.embl-heidelberg.de](http://smart.embl-heidelberg.de)) [38,39] revealed three 341  
 coiled-coil domains at amino acid positions 33–192, 218–399 342  
 and 420–454 (Fig. 2). The presence of coiled-coil domains is 343  
 known to be a characteristic feature of centrosomal proteins 344  
 [40]. In addition, a search using the PROSITE database [41] 345  
 revealed twelve potential casein kinase II phosphorylation 346  
 sites, seven protein kinase C phosphorylation sites, a cAMP-/ 347  
 cGMP-dependent protein kinase phosphorylation site, a tyr- 348  
 osine kinase phosphorylation site, three N-glycosylation sites, 349  
 and an N-myristoylation site (Table 1). Multiple phosphoryla- 350  
 tion sites are also typical for centrosomal proteins [42], while 351  
 the N-myristoylation site indicates interaction with mem- 352  
 branes, presumably reflecting a relation to Golgin [43]. 353

### 354 The presence of Crp<sup>F46</sup> in HeLa cells

The polypeptide recognized by the F46 serum on immunoblots 355  
 is only  $\sim 60$  kDa, while the homologous Golgin-245 has a 356  
 molecular mass of 245 kDa. Therefore it was necessary to 357  
 confirm that a recombinant Crp<sup>F46</sup>, derived from a cDNA ob- 358  
 tained on the basis of the MS/MS sequencing, does correspond 359  
 to the endogenous Crp<sup>F46</sup> and is recognized by the F46 serum. 360  
 We designed primers according to the first and last polypep- 361  
 tides of the MS/MS result (Fig. 2) and used RT-PCR and HeLa 362  
 total RNA as a template to obtain Crp<sup>F46</sup> cDNA. The cDNA was 363  
 then used to construct a GST-Crp<sup>F46</sup> chimeric gene, and GST- 364  
 Crp<sup>F46</sup> fusion protein was expressed using pGEX-2Z-Crp<sup>F46</sup> 365  
 expression vector transformed into *Escherichia coli*. The recom- 366  
 binant proteins was purified and submitted for preparation of 367  
 monoclonal antibodies. Immunoblots with endogenous pro- 368  
 teins extracted from HeLa cells showed that both anti-Crp<sup>F46</sup> 369  
 monoclonal antibody and the F46 serum gave positive 370  
 immunoreactions at the expected locations (Fig. 3). Further- 371  
 more, both antibodies also gave positive immunoreactions 372  
 with the recombinant protein. Therefore, the cloned Crp<sup>F46</sup> 373

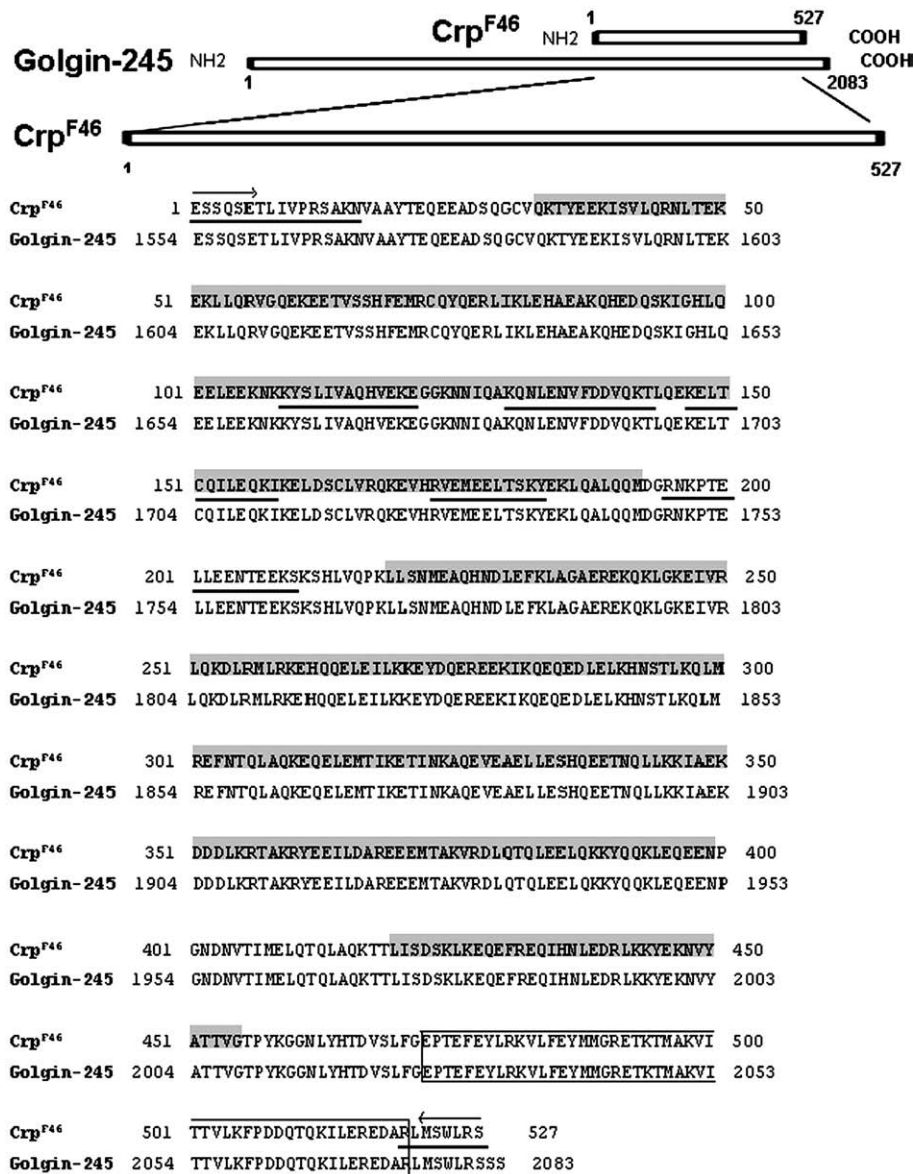


**Fig. 2 – Crp<sup>F46</sup> is highly homologous to a 527 amino acids sequence of the C-terminal domain of Golgin-245. Amino acid sequences were obtained by MS/MS of a protein immunoprecipitated with F46 serum, and aligned with Golgin-245 sequence using BLASTN. SMART analysis identified three coiled-coil domains (shaded) at specified amino acid positions. Amino acid sequences of peptides identified MS/MS are underlined. Amino acids corresponding to GRIP domain are boxed. Arrows indicate the starting positions of segments used for the design of forward and reverse degenerate primers.**

374 does indeed correspond to the endogenous Crp<sup>F46</sup> protein  
 375 originally detected by the F46 serum.

376 **Crp<sup>F46</sup> is a splice variant of Golgin-245**

377 In order to determine if Crp<sup>F46</sup> is a splice variant of Golgin-245 or  
 378 encoded by a distinct gene, we constructed a pcDNA3.1+  
 379 antisense *golgin-245* vector. This vector targets the nucleotides  
 380 320–1627 bp of the N-terminus of *golgin-245*, which is outside the  
 381 Crp<sup>F46</sup> domain. The antisense vector, or an empty pcDNA3.1+  
 382 *neo* vector as a control, were transfected into HeLa cells, and  
 383 clonal cell lines stably expressing the respective vectors were  
 384 established using geneticin (G418) selection. Western blot  
 385 analysis of protein extracts from the two clonal cell lines

386 showed that the antisense *golgin-245* knocked down the ex-  
 387 pression of Golgin-245 and also the expression of Crp<sup>F46</sup> (Fig. 4).  
 388 In contrast, transformation with an antisense Crp<sup>F46</sup> RNA vector  
 389 showed that only the CrpF46 was depleted but Golgin-245 was  
 390 still present. We therefore conclude that Crp<sup>F46</sup> is the product of  
 391 splicing of *golgin-245*, and not encoded by a distinct gene.

392 It should be noted that the 527 amino acid sequence at the  
 393 C-terminus of Golgin-245 that correspond to Crp<sup>F46</sup> includes a  
 394 GRIP domain (residues 2026–2070; Fig. 2), which is necessary,  
 395 though not sufficient, for localization to the Golgi apparatus  
 396 [44,45]. Unfortunately our MS/MS sequencing did not cover the  
 397 site of the potential GRIP domain and therefore we have no  
 398 direct evidence that this domain is either present or absent in  
 399 the Crp<sup>F46</sup>. However, our immunostaining assays (Figs. 5, 6, 8,

**Table 1 – Putative protein modification sites identified by searching the PROSITE database**

Putative modification site	Amino acid positions	Amino acid motif
Casein kinase II phosphorylation	3–6	SqsE
	21–24	TeqE
	35–38	TyeE
	48–51	TekE
	67–70	ShfE
	143–146	TlqE
	181–184	SkyE
	221–224	SnmE
	317–320	TikE
	335–338	ShqE
	381–384	TqlE
	406–409	TimE
Protein kinase C phosphorylation	13–15	SaK
	48–50	TeK
	180–182	TsK
	295–297	TlK
	317–319	TiK
	357–359	TaK
	373–375	TaK
cAMP- and cGMP-dependent protein kinase phosphorylation	108–111	KKyS
Tyrosine kinase Phosphorylation	443–450	Kky.EknV
N-glycosylation	46–49	NLTE
	293–296	NSTL
	404–407	NVTI
N-myristoylation	122–127	GGknNI

and 10) consistently showed centrosomal, not Golgi, localization throughout interphase. Further exploration will be required to determine the mechanism of Crp<sup>F46</sup> targeting to the centrosome.

#### Cell-cycle-dependent localization of Crp<sup>F46</sup> to the centrosome in synchronized HeLa cells

To determine the subcellular localization and dynamic distribution of Crp<sup>F46</sup> during the cell cycle, we synchronized HeLa cells and processed them for immunofluorescence microscopy using the anti-Crp<sup>F46</sup> monoclonal antibody. During interphase, the immunoreactive material consistently localized to one or two bright dots in the cytoplasm adjacent to the nucleus (Figs. 5A,B). In many cells at G1/S phase, the single bright dot appeared to be dividing into two dots, which were initially interconnected but eventually became completely separated. Once the nucleus entered mitosis, however, the two bright dots of Crp<sup>F46</sup> were replaced by a weaker, though distinct, punctuate signal throughout the cytoplasm. This indicates that the immunoreactive material dissociates from the centrosomes and becomes fragmented and scattered through the cytoplasm.

The only known cellular structure that behaves similarly to the Crp<sup>F46</sup> during interphase is the centrosome, which typically shows one- or two-dot pattern in the perinuclear cytoplasm. To test the relation of the Crp<sup>F46</sup> to the centrosome, we performed double immunolabeling using the anti-Crp<sup>F46</sup> monoclonal antibody and anti- $\gamma$ -tubulin polyclonal antibody in order to locate the centrosome. Throughout interphase, the Crp<sup>F46</sup> was indeed found to co-localize with  $\gamma$ -tubulin and hence the

centrosomes (Fig. 5C). Cells at G1 showed a single Crp<sup>F46</sup> dot, typical of centrosomes during G1 and early S phases. A pair of closely connected dots appeared during S phase, and two separate dots became clearly visible during late S and G2 phases. At the onset of mitosis, when the two centrosomes moved to the opposite poles of the cell, the bright, compact Crp<sup>F46</sup> dots began to disappear. A weaker but distinct punctuate fluorescent signal again became scattered throughout the cytoplasm during mitosis, without any specific co-localization with the pair of centrosomes marked with the  $\gamma$ -tubulin label. Nevertheless, following cytokinesis the punctate cytoplasmic staining disappeared and a distinct, compact Crp<sup>F46</sup> dot again re-appeared together with the single centrosome in each of the two daughter cells, suggesting re-association of the punctate signal with the centrosome. Thus the Crp<sup>F46</sup> accompanies the centrosome during its typical duplication and subcellular localization during interphase, although it disperses during mitosis and re-appears again during the G1 phase of the next cell cycle as a compact dot accompanying the single centrosomes in each daughter cell.

#### Crp<sup>F46</sup> deletion fragment (aa 323–530) containing coiled-coil III confers localization to the centrosome

As the first step towards elucidating the mechanism of targeting the Crp<sup>F46</sup> to the centrosome, we used PCR specific primers together with Crp<sup>F46</sup> cDNA as a template to prepare three deletion fragments corresponding to the regions of the three coiled-coil domains (Fig. 6A). The fragments were ligated into the expression vector pEGFP-C3 and the recombinant vector transiently transfected into HeLa cells. Cells expressing GFP fusion protein were counter-stained with

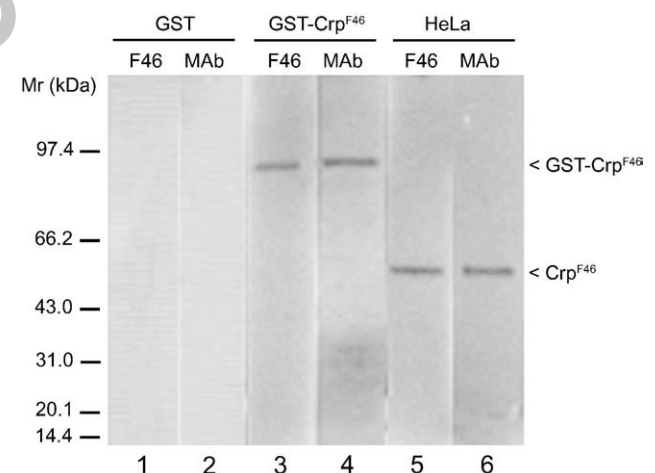


**Fig. 3 – Western blot analysis of HeLa proteins and recombinant Crp<sup>F46</sup> using F46 serum and an anti-Crp<sup>F46</sup> monoclonal antibody. Total proteins from E. coli expressing GST protein (lanes 1 and 2) or Crp<sup>F46</sup> fusion protein (lanes 3 and 4), and total proteins from HeLa cells (lanes 5 and 6) were separated by SDS-PAGE, transferred onto nitrocellulose membrane, and probed with F46 serum (F46) or anti-Crp<sup>F46</sup> monoclonal antibody (MAb). Arrows indicate immunoreactive bands at the expected M<sub>r</sub> in protein extracts containing either recombinant GST-Crp<sup>F46</sup> or endogenous Crp<sup>F46</sup>.**

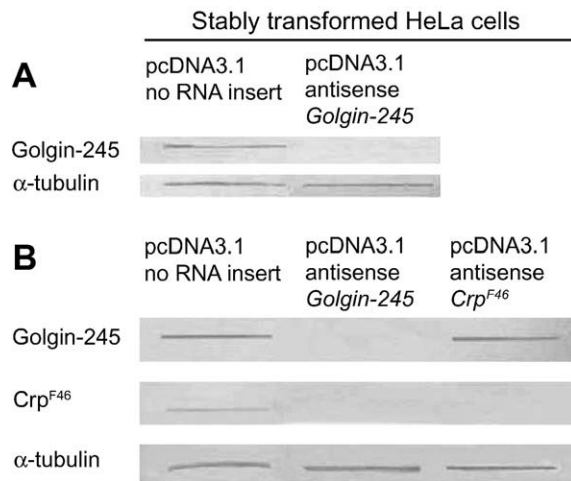


**Fig. 4 – Knockdown of Golgin-245 by antisense golgin-245 also blocks the expression of Crp<sup>F46</sup>.** (A) Protein extracts were prepared from HeLa cell lines transformed with pcDNA3.1+ antisense golgin-245 RNA or with the empty pcDNA3.1+ vector as a control, separated by SDS-PAGE, and probed by Western blotting using antibody against Golgin-245. While the protein extract from the control cell line showed normal levels of Golgin-245, expression of this protein was effectively knocked down in the cell line stably transformed with the antisense golgin-245 RNA vector. (B) Stable transformation with antisense Crp<sup>F46</sup> RNA knocked down the expression of Crp<sup>F46</sup> but did not deplete Golgin-245. Probing with an antibody against  $\gamma$ -tubulin confirms equal protein loading.

antibody against  $\gamma$ -tubulin to identify the centrosome, and examined by confocal microscopy. Only the cells expressing either intact Crp<sup>F46</sup> or the (aa 323–530) fragment, which contains the C-terminal coiled-coil domain III at residues 420–454, showed typical centrosomal localization in interphase cells (Fig. 6B). By contrast, cells expressing the fragments (aa 1–241) or (aa 127–426), which contain coiled-coil domains I and II, gave only non-specific cytoplasmic GFP signal similar to that in cells expressing the control EGFP. Therefore centrosomal localization is conferred by the Crp<sup>F46</sup> (aa 323–530) fragment, most likely through the coiled-coil domain III.

#### Interaction of Crp<sup>F46</sup> with $\gamma$ -tubulin and with the centrosomal protein kinase Plk1

To test whether Crp<sup>F46</sup> interacts with any known centrosomal proteins, we performed co-immunoprecipitation using the anti-Crp<sup>F46</sup> monoclonal antibody and total protein extract of HeLa cells. Analysis of the immunocomplex by SDS-PAGE and Western immunoblotting using anti- $\gamma$ -tubulin polyclonal antibody revealed that the complex indeed contains  $\gamma$ -tubulin (Fig. 7). The Crp<sup>F46</sup> therefore does interact with  $\gamma$ -tubulin, consistent with the co-localization of the two proteins at the centrosome shown by the immunofluorescence microscopy above.

The cell-cycle-dependent association of Crp<sup>F46</sup> with the centrosome suggests that the mechanism is likely to involve protein phosphorylation, possibly by a known centrosomal kinase such as Plk1 [7,8]. To test this hypothesis, we probed

nitrocellulose protein transfers of the Crp<sup>F46</sup> immunocomplex with an anti-Plk1 antibody. The Western immunoblot revealed a positive reaction, indicating that Crp<sup>F46</sup> is indeed a target of Plk1. Likewise, reciprocal immunoprecipitation using antibodies against PLK1 or  $\gamma$ -tubulin also gave complexes that consistently contained all three proteins, confirming the three proteins interact. By contrast, immunoprecipitation using anti-Golgin-245 did not form complexes with any of these proteins.

#### Antisense Crp<sup>F46</sup> knockdown inhibits the growth and proliferation of HeLa cells

In order to examine the functional role of Crp<sup>F46</sup>, we inserted an antisense RNA for the whole Crp<sup>F46</sup> coding sequence into pXJ41 expression vector and transfected the resulting construct into HeLa cells. A clonal cell line in which the Crp<sup>F46</sup> was stably transformed was established by using geneticin (G418) selection [46], and silencing was verified by Western blotting and immunofluorescence microscopy using anti-Crp<sup>F46</sup> monoclonal antibody. Antisense RNA effectively knocked down the expression of Crp<sup>F46</sup> (Fig. 8A), and it also abolished the typical centrosomal association of the Crp<sup>F46</sup> (Fig. 8B). A clonal cell line transfected with the control vector pXJ41 alone showed no specific silencing response.

After several passages of the antisense-Crp<sup>F46</sup> cell line, an increasing number of cells showed dramatic changes in their morphology. The aberrant cells either became abnormally large and multinucleate (Fig. 9A, arrow 2; see also Fig. 10A) or unusually long and narrow (Fig. 9A, arrow 3). The silencing inhibited the growth and proliferation of cells by about 15% after every passage (Fig. 9C). With continuous subculturing, many cells began to fragment and form conglomerations, indicating that cell growth was severely disrupted (Fig. 9A, arrow 4). Coenocytes containing several mini-nuclei also appeared (Fig. 9A, arrow 1). These results suggest that silencing of Crp<sup>F46</sup> gradually becomes more effective during continuous subculturing. Eventually, many cells have stopped growing and entered apoptosis, resulting in progressive accumulation of cell debris. The ability of the antisense-Crp<sup>F46</sup> cell line to subculture was also greatly reduced. Flow cytometry analysis revealed that the cell cycle typically stalled at S phase, with marked reduction in the proportion of cells at G2 (Fig. 9D).

#### The formation of poly-centrosomal and multinucleate cells in antisense-Crp<sup>F46</sup> cell line

In order to analyze in more detail the subcellular effects of silencing the Crp<sup>F46</sup>, we processed antisense-Crp<sup>F46</sup> cells and control cells (pXJ41 no RNA insert) for immunofluorescence labeling with anti-Crp<sup>F46</sup> monoclonal antibody (green) and counter-staining with PI to label DNA (red) (Fig. 10A). Confocal microscopy revealed that silencing of Crp<sup>F46</sup> caused the formation of coenocytic cells with numerous mini-nuclei and also multinucleate cells, as well as apoptotic cells with aberrant chromatin condensation or fragmented nuclei. To determine if depletion of Crp<sup>F46</sup> also affected the centrosome, we labeled the cells with anti- $\gamma$ -tubulin polyclonal antibody. Many cells displayed poly-centrosomal morphology (Fig. 10B).

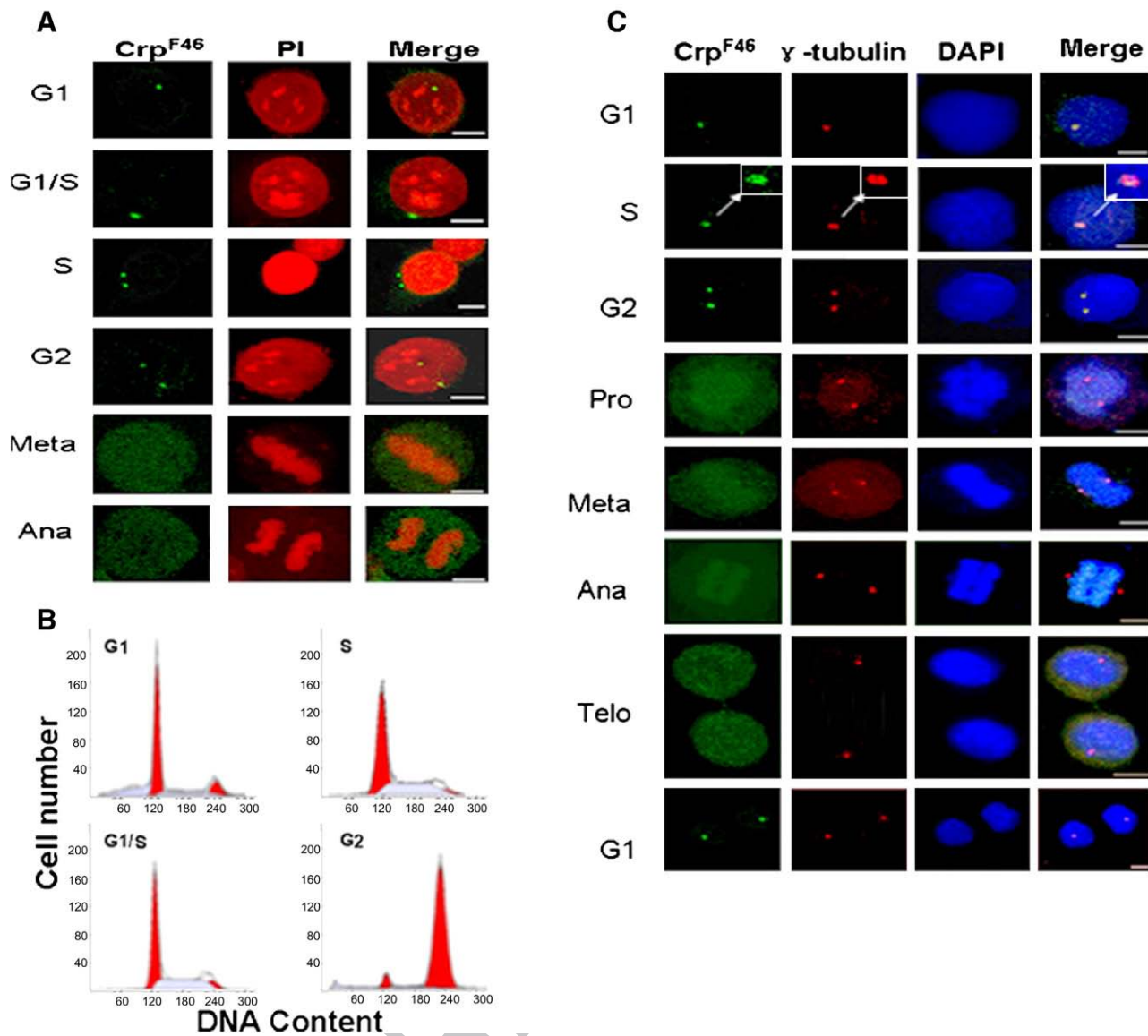


**Fig. 5** – Subcellular localization of Crp<sup>F46</sup> in synchronized HeLa cells, visualized by immunofluorescence labeling and confocal laser-scanning microscopy. HeLa cells were synchronized by culturing in DMEM containing 10% FCS and 2 mM TdR for specific periods (see text). The cells were processed for immunolocalization of Crp<sup>F46</sup> using anti-Crp<sup>F46</sup> monoclonal antibody (green) and counter-staining with propidium iodide (PI) to show DNA (red). Individual stages of the cell cycle were determined by FACS analysis. (A) Separate colour images and the merge images show that Crp<sup>F46</sup> was clearly visible during interphase when it formed one or two bright dots in the cytoplasm next to the nucleus. The bright dots disappeared at the onset of mitosis, although a weaker, punctuate signal became dispersed throughout the cytoplasm. (B) Graphs showing DNA content and cell-cycle phase determined by FACS analysis. (C) Colocalization of Crp<sup>F46</sup> with  $\gamma$ -tubulin as a centrosomal marker was examined in synchronized cells that were double-labeled with anti-Crp<sup>F46</sup> monoclonal antibody (green) and anti- $\gamma$ -tubulin polyclonal antibody (red), and DNA was counter-stained with DAPI (blue). Separate colour images and the merge images show that the Crp<sup>F46</sup> co-localized with the centrosomes throughout interphase. At the onset of mitosis the bright dots were replaced by a weaker, punctuate signal scattered throughout the cytoplasm. Following cytokinesis, a compact dot of Crp<sup>F46</sup> appeared again in co-localization with the single centrosome in each daughter cell in G1. Scale bars in A and B, 10  $\mu$ m.

540 Furthermore, immunostaining with anti- $\alpha$ -tubulin polyclonal  
 541 antibody revealed dramatic changes in spindle structure and  
 542 organization, producing multipolar mitotic spindles (Fig. 10C).  
 543 The formation of multipolar spindles and asymmetric mitoses  
 544 are likely to produce coenocytes with mini-nuclei as noted

above. In the apoptotic multinucleate cells, the centrosomes  
 545 generally became smaller and numerous, indicating that  
 546 apoptosis was the result of a failure to complete the M  
 547 phase. These results are consistent with the decline in cell  
 548 growth and proliferation as documented in Fig. 9. 549

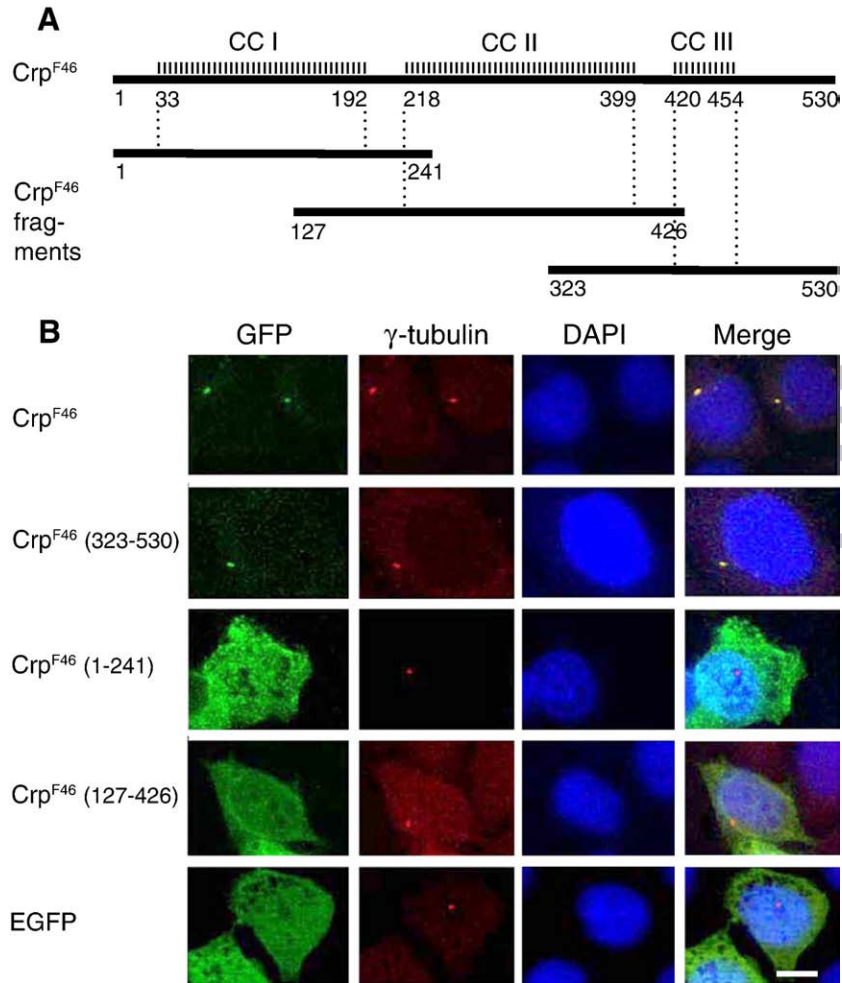


**Fig. 6** – Deletion-analysis identification of a Crp<sup>F46</sup> domain that confers centrosomal localization. (A) Diagram of amino acid residues defining the positions of Crp<sup>F46</sup> of coiled-coil domains CC I, CC II, and CC III, and the locations of corresponding deletion fragments. (B) Confocal images of HeLa cells expressing recombinant vectors pEGFP-C3 fused with the whole Crp<sup>F46</sup> sequence or its deletion fragments. The HeLa cells were transiently transformed with the recombinant vectors and maintained for 2 days. Cells expressing GFP fusion protein were counter-stained with  $\gamma$ -tubulin antibody and TRITC-conjugated second antibody. Only cells expressing the Crp<sup>F46</sup> (aa 323–530) deletion fragment, which contains the coiled-coil III domain, showed typical centrosomal localization similar to that seen with the intact Crp<sup>F46</sup>. Cells expressing the deletion fragments (aa 1–241) or (aa 127–426) showed general cytoplasmic signal. Scale bar, 10  $\mu$ m.

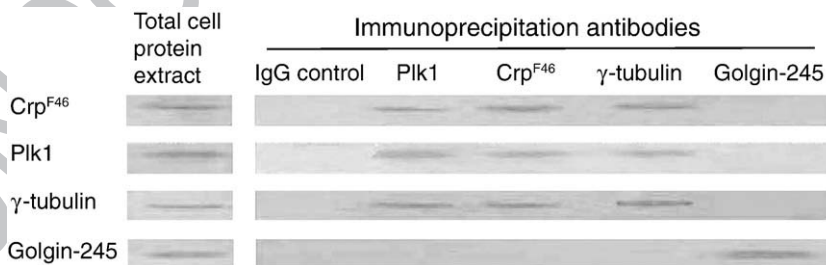


**Fig. 7** – Interaction of Crp<sup>F46</sup> with  $\gamma$ -tubulin and with the protein kinase Plk1. Total protein extracts from HeLa cells were incubated with each of antibodies against Crp<sup>F46</sup>, Plk1, or  $\gamma$ -tubulin, the individual immunoprecipitated complexes then separated by SDS-PAGE, transferred to nitrocellulose blots and probed with specified antibodies. Immunoprecipitation using anti-Crp<sup>F46</sup> monoclonal antibody followed by Western immunoblotting gave positive reactions with both anti-Plk1 and anti- $\gamma$ -tubulin, indicating the three proteins interact as a complex. Reciprocal immunoprecipitation with antibodies against Plk1 or anti- $\gamma$ -tubulin also showed that the three proteins form a complex. Immunoprecipitation with antibody against Golgin-245 did not form complexes with any of these proteins, and immunoprecipitation with an IgG control was negative.

## Discussion

551

552 In this study we identified a novel centrosome-related protein,  
553 Crp<sup>F46</sup>, by using an anti-serum F46 from a patient suffering  
554 from progressive systemic sclerosis. The protein attracted our  
555 attention because of its unique cell-cycle-dependent localiza-  
556 tion to the centrosome. We characterized the protein by im-  
557 munoprecipitation and Western blot using the F46 serum and  
558 tandem mass spectrometry (MS/MS) sequencing. Its apparent  
559 molecular mass is ~60 kDa, and its predicted amino acid  
560 sequence is highly homologous to the C-terminal portion of  
561 the protein Golgin-245 using BLAST search of the NCBI/EMBL  
562 databases. Western blot of HeLa proteins using a monoclonal  
563 antibody raised against a recombinant protein derived from  
564 the MS/MS sequencing again showed an immunoreactive band  
565 of ~60 kDa, confirming that Crp<sup>F46</sup> is indeed present in HeLa  
566 cells. Immunostaining assay with the anti-Crp<sup>F46</sup> monoclonal  
567 antibody revealed one or two sharp dots near the nuclear

envelope at interphase, indicating that Crp<sup>F46</sup> most likely  
localizes to the centrosome. Double-labeling experiments  
using synchronized HeLa cells and anti- $\gamma$ -tubulin polyclonal  
antibody showed that Crp<sup>F46</sup> co-localized with  $\gamma$ -tubulin during  
interphase but not in mitosis. Therefore, the Crp<sup>F46</sup> is a novel  
centrosome-related protein that dissociates from the centro-  
somes and disperses into the cytoplasm at the onset of mitosis.

According to the deletion fragment analysis, the centroso-  
mal localization of Crp<sup>F46</sup> is conferred by its C-terminal  
fragment (aa 323–530), most likely through the coiled-coil  
domain III located at residues 420–454. Many centrosomal  
proteins, such as TAX1BP2, ninein, rootelin, Cep135, and OFD1,  
contain coiled-coil domains, and mutations within these  
domains abolish centrosomal localization [40,47–50]. The  
coiled-coil domain itself may therefore be sufficient to confer  
localization to the centrosome. Some centrosomal proteins,  
such as TAX1BP2, CG-NAP, and pericentrin, can also interact  
with other centrosomal proteins [40,51,52]. Since our co-  
immunoprecipitation experiment demonstrated that Crp<sup>F46</sup>  
interacts with  $\gamma$ -tubulin, this interaction may serve as a  
piggyback mechanism for centrosomal localization during  
interphase. The cell-cycle-dependent association of Crp<sup>F46</sup>  
with the centrosome is likely to be regulated by phosphoryla-  
tion, possibly through interaction with the protein kinase Plk1  
as indicated by our co-immunoprecipitation experiment.

Golgin-245 is known to localize specifically to the Golgi  
apparatus, which performs many unique processes [53].  
Despite the distinct localization and function of the Golgin-  
245 and the Crp<sup>F46</sup>, the relationship between the Golgi  
apparatus and the centrosomes is very close as indicated by  
a list of intimate interactions: (a) The centrosome serves a  
crucial role in the establishment of the Golgi apparatus, and  
interaction of the Golgi apparatus with microtubules is  
important for reconstruction and transport of the Golgi  
complex following mitosis and cytokinesis; (b) GMAP-210  
(Golgi microtubule-associated protein 210) connects cis-Golgi  
network to the minus ends of centrosome-nucleated micro-  
tubules with its respectively N-terminus and C-terminus [54];  
(c) CG-NAP (centrosome and Golgi localized PKN-associated  
protein), locates at centrosome or Golgi apparatus at different  
phases of the cell cycle [55]; (d) centrosomin's beautiful sister  
(cbs), a *trans*-Golgi protein, has been found to relate to mature  
centrosomes [56]; and (e) three members of AKAP350 family  
(AKAP350A, AKAP350B, and AKAP350C), which are the pro-  
ducts of a multiply spliced AKAP, localize to the centrosome  
and/or the Golgi apparatus after C-terminal splicing events  
[57]. Thus a protein can contain more than one targeting  
domain, and splicing events can generate several members  
that have distinct subcellular localizations and functions. This  
may be particularly true for proteins containing coiled-coil  
domains [75].

Our transformation of HeLa cells with antisense *golgin-245*  
RNA apparently depleted both Golgin-245 and Crp<sup>F46</sup>. There-  
fore it is likely that Crp<sup>F46</sup> is the product of alternative splicing  
of mRNA transcribed from the entire open reading frame  
of *golgin-245*, although the process may also involve post-  
translational modifications in the coiled-coil III domain. Such  
a splice variant could still include the GRIP domain. Although  
this domain is necessary for binding to Golgi, it is not  
sufficient because the binding also requires hierarchical

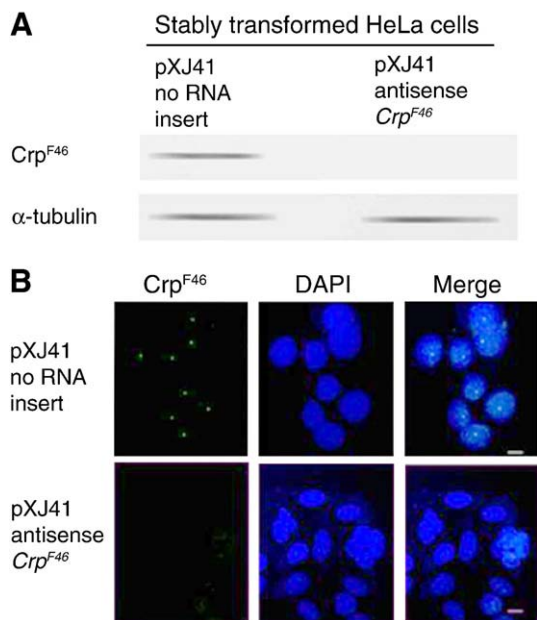


**Fig. 8 – Characterization of a stable antisense-Crp<sup>F46</sup> HeLa cell line. (A)** Western blot analysis of protein extracts of control cell line (pXJ41 no RNA insert) and antisense-Crp<sup>F46</sup> cell line using anti-Crp<sup>F46</sup> specific monoclonal antibody and  $\alpha$ -tubulin antibody to check for equal protein loading. Whereas the control cells showed a normal level of Crp<sup>F46</sup>, expression of Crp<sup>F46</sup> was effectively knocked down in the antisense-Crp<sup>F46</sup> cell line. **(B)** Confocal immunofluorescence images of control cells (pXJ41 no RNA insert) and antisense-Crp<sup>F46</sup> cells labeled with anti-Crp<sup>F46</sup> specific antibody (green) and counter-stained with DAPI to label DNA (blue). Merge images show that the silencing of Crp<sup>F46</sup> abolished the normal bright staining of centrosomal dots, and a number of cells became multinucleate. Control cells (pXJ41 no RNA insert) appeared normal, without any silencing defects. Scale bars, 10  $\mu$ m. (For interpretation of the references to colour in this figure legend, the reader is referred to the web version of this article.)

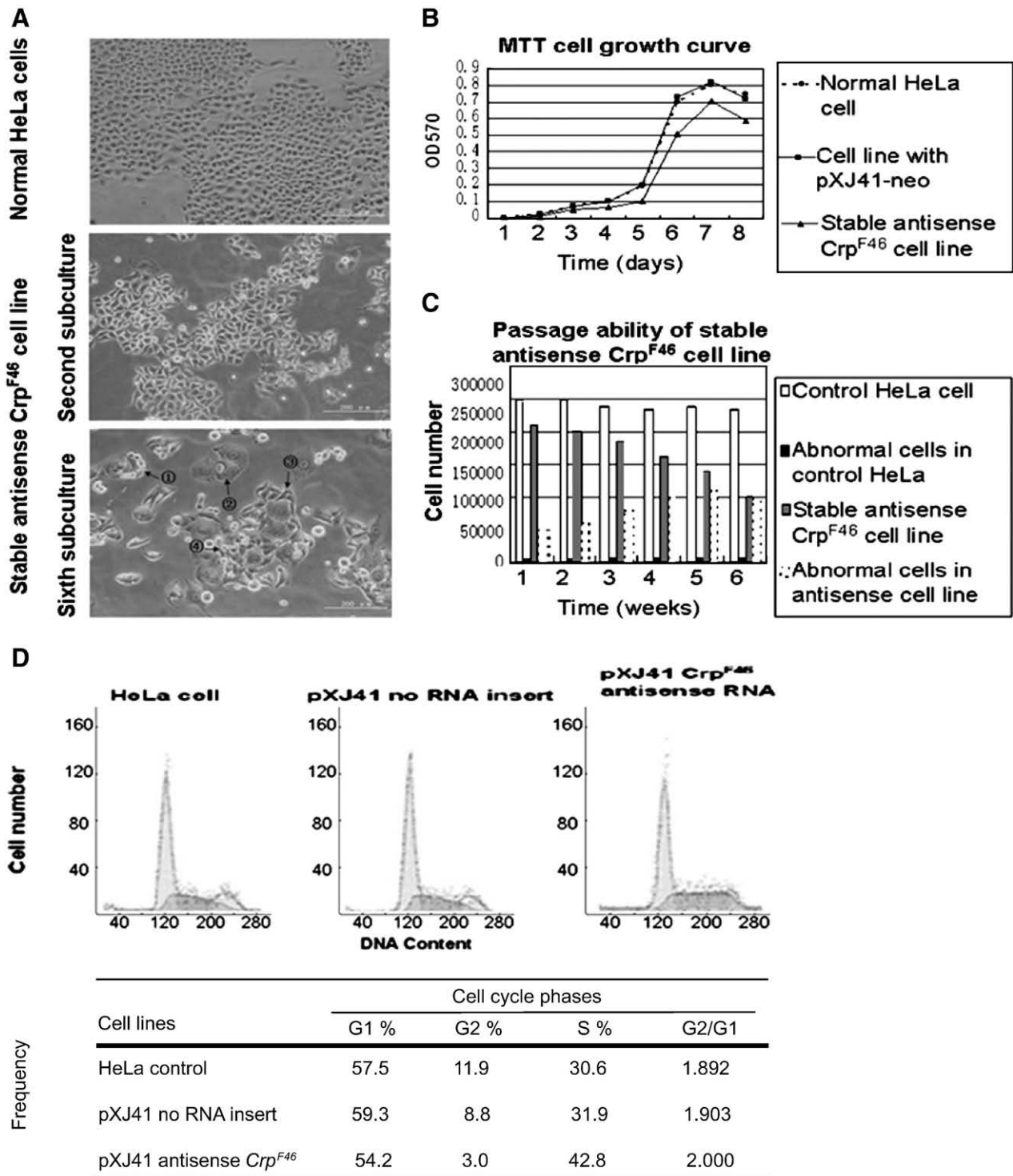


**Fig. 9** – Mitotic defects and disruption in cell-cycle progression in stable antisense-Crp<sup>F46</sup> HeLa cell line. (A) Accumulation of morphological abnormalities (arrows) with repeated subculturing (passages) of the antisense-Crp<sup>F46</sup> cell line. (B) Cell growth curves, determined by the MTT method, showing that cell growth and proliferation in the antisense-Crp<sup>F46</sup> cell line was inhibited by ~15%. (C) Declining passage vigor and increasing frequency of morphological abnormalities with repeated subculturing of the antisense-Crp<sup>F46</sup> cell line. Wt cell line and antisense-Crp<sup>F46</sup> cell line in exponential phase of growth were repeatedly subcultured at weekly intervals over 6 weeks and grown for 4 days, and the number of normal and abnormal cells determined in each cell line. In the wt cell line, the number of normal cells and the relatively low frequency of abnormal cells remained unchanged over the 6 passages. In contrast, in the antisense-Crp<sup>F46</sup> cell line the total number of normal cells gradually declined and the number of abnormal cells increased with each passage. (D) Flow cytometry analysis of the antisense-Crp<sup>F46</sup> cells showed that the cell cycle was prominently stalled at S phase.

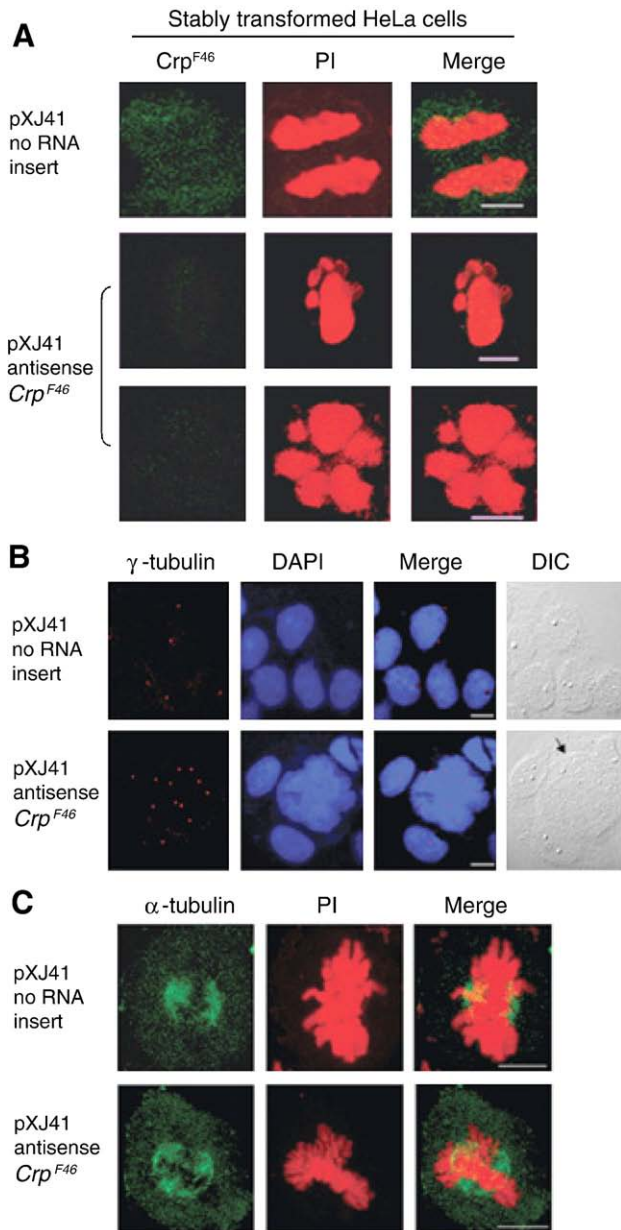


**Fig. 10 – Confocal immunofluorescence microscopy of a stable antisense-Crp<sup>F46</sup> cell line. (A)** Immunofluorescence images of control cells (pXJ41 no RNA insert) and antisense-Crp<sup>F46</sup> cells probed with anti-Crp<sup>F46</sup> monoclonal antibody (green) and counter-stained with PI to show DNA (red). Expression of Crp<sup>F46</sup> was effectively knocked down in the antisense-Crp<sup>F46</sup> cells, compared with the normal scattered punctate staining in a control cell at anaphase. The silenced cell line typically contained multinucleate and coenocytic cells, or apoptotic cells with aberrant chromatin condensation and fragmented nuclei. **(B)** Multiple centrosomes, identified by staining with anti- $\gamma$ -tubulin polyclonal antibody (red). Counter-staining DNA with DAPI (blue) and DIC reveal a large, multinucleate, poly-centrosomal cell (arrow). **(C)** Formation of a multipolar mitotic spindle in an antisense-Crp<sup>F46</sup> cell, revealed by staining with anti- $\alpha$ -tubulin monoclonal antibody (green) and PI (red). Scale bars in A–C, 10  $\mu$ m. (For interpretation of the references to colour in this figure legend, the reader is referred to the web version of this article.)

interactions with other proteins and phospholipids that contribute synergistically to Golgi targeting [45]. Clearly, our results show that Crp<sup>F46</sup> has its unique localization to the centrosome during interphase and performs a function independent from the Golgi. The exact mechanism of origin of Crp<sup>F46</sup> remains to be established.

Another unique feature of the Crp<sup>F46</sup> is its cell-cycle dependent association with the centrosome. The dissociation of Crp<sup>F46</sup> from the daughter centrosomes at the onset of mitosis is most likely a part of ‘centrosome maturation’ in preparation for mitosis [58]. During this process, a number of proteins are recruited to the centrosomes as a result of changes in phosphorylation status, largely involving proteins that increase the microtubule nucleation activity required for the establishment of the microtubule spindle. At the same time, the Golgi apparatus fragments and disperses from the nuclear region into the cytoplasm [59]. It appears that the Crp<sup>F46</sup> follows a similar behavior, dissociating from the centrosome and scattering through the cytoplasm, a process that most likely involves changes in phosphorylation status. An example of such behavior is Nlp (ninein-like protein), which becomes phosphorylated by Plk1 (polo-like kinase 1) and dissociates from the centrosomes at G2/M transition and then redistributes into the cytoplasm during mitosis [60,61]. Similarly, Chk1 (checkpoint kinase 1) localizes specifically to interphase, but not mitotic, centrosomes [62]. Co-immunoprecipitation of Crp<sup>F46</sup> with Plk1 in our experiments indicates that the cell-cycle-dependent association of Crp<sup>F46</sup> with the centrosome likewise involves phosphorylation, consistent with its abundant potential phosphorylation sites.

Phosphorylation on Ser/Thr-Pro sites is a major mechanism regulating many events in cell proliferation and differentiation, including centrosome duplication. Many centrosomal proteins, such as centrin, NPM/B23, Nlp, and Pin1 [13,56,68,69], are known to localize on, or dissociate from, the centrosome and to regulate centrosome duplication with phosphorylation as the prerequisite step.

Our results with stable transformation of HeLa cells with antisense-Crp<sup>F46</sup> RNA show that Crp<sup>F46</sup> may also play an active role in cell proliferation and influence cell-cycle progression. Thus, Crp<sup>F46</sup> depletion inhibited cell growth and proliferation, reduced the effectiveness of cell subculturing as the proportion of abnormal cells increased after every passage, and the cell cycle was stalled at S phase. Furthermore, the depletion also caused various morphological changes, including abnormalities in cell volume and the emergence of multinucleate cells containing 2–6 nuclei. Thus the cell-cycle progression was not only inhibited but also seriously disrupted in various ways.

In current view, the centrosome plays an important role not only in microtubule nucleation but also in cell-cycle regulation [63]. Centrosome duplication is closely coupled with other cell cycle events, especially DNA synthesis [64]. Abnormalities in centrosome-associated proteins like pin1, Rad6, and cyclin D1 can cause centrosome re-duplication and affect the regulation of the cell cycle. Such abnormalities lead to the formation of multinucleate cells, cells with multipolar spindles, mitotic spindle abnormalities, aneuploidy, chromosome instability, oncogenesis, and other defects [13,14,65]. Similarly, the antisense depletion of Crp<sup>F46</sup> in our experiments included alteration in centrosomal number, formation of multipolar spindles, 687

688 and the formation of coenocytes as a result of failed cytokin-  
689 esis. Interestingly, the Crp<sup>F46</sup> association with the centrosome  
690 is limited to interphase, suggesting it may be involved in cen-  
691 trosome duplication. Replication of the centrosome is induced  
692 by the activity of cyclin E-Cdk2 complex at G1/S phase [66,67],  
693 which is regulated by proteins such as p21 or cki-2 [17]. It seems  
694 plausible that Crp<sup>F46</sup> could modulate the activity of these or  
695 other proteins that participate in centrosome duplication.

696 It is unknown exactly how Crp<sup>F46</sup> may participate in the  
697 regulation of the cell cycle. However, its specific localization to  
698 the centrosome in interphase is consistent with its proposed  
699 role in centrosome duplication. Since the centrosome repli-  
700 cates during the S phase, there is a direct relationship between  
701 poly-centrosomes and stalling of the cell cycle at the S phase,  
702 both of which can be caused by silencing the Crp<sup>F46</sup>. Similarly,  
703 recent research revealed that the expression of Cdc25<sup>string</sup>,  
704 which drives cells into mitosis, is required for the completion  
705 of daughter centriole assembly and ensuring that the centro-  
706 some replicates only once in the normal cell cycle in *Drosophila*  
707 cells [70,71]. Recent research has also shown that components  
708 of the large  $\gamma$ -tubulin ring complex participate in the spindle  
709 assembly checkpoint [72]. Since Crp<sup>F46</sup> co-localizes and inter-  
710 acts with  $\gamma$ -tubulin, it is a likely candidate for a role in cell-  
711 cycle progression.

712 The mechanism of cell proliferation remains a hot spot in  
713 cancer research. Cancer cells typically have abnormal centro-  
714 some number, and the absence of tumor suppressor proteins  
715 such as P53 can cause centrosome re-duplication [73]. Silen-  
716 cing of Crp<sup>F46</sup> has a similar effect. Another potential player in  
717 cancer cells is the centromere. Since the centromere/kineto-  
718 chore complex connects the chromosome to microtubules,  
719 and the centrosome acts as a microtubule-organizing center,  
720 there is likely to be mutual relationship between centrosome  
721 re-duplication, formation of multipolar spindles, centromere  
722 abnormalities, and abnormal chromosomal number or struc-  
723 tural instabilities [74]. Investigation of centromere proteins in  
724 the antisense Crp<sup>F46</sup> cell line will be required in order to  
725 elucidate the role of Crp<sup>F46</sup> in the mechanism of chromosome  
726 separation and morphological abnormalities in the cell.

727 In conclusion, our research demonstrates a role of a novel  
728 centrosomal protein Crp<sup>F46</sup> in cell-cycle dynamics. Further  
729 investigation of the Crp<sup>F46</sup> is likely to produce new information  
730 about the role of the centrosome in cell-cycle regulation,  
731 mitosis and cytokinesis, possibly benefiting the treatment of  
732 cancer.

### 734 Acknowledgments

735 We thank Drs. Yongzhe Li and Jingtao Cui (Peking Union  
736 Medical College, Chinese Academy of Medical Science, China)  
737 for providing autoimmune-sera, Dr. Xiaoyu Zhu (Beijing  
738 Normal University, China) for a gift of pXJ41-neo vector, Dr.  
739 Wanjie Li (Beijing Normal University, China) for a gift of ex-  
740 pression vector pEGFP-C3, Professor Marvin J. Fritzler (Depart-  
741 ment of Biochemistry and Molecular Biology, University of  
742 Calgary, Calgary, Alberta, Canada) for kindly providing Golgin-  
743 245 antibody, and Dr. Yue Wang (Institute of Molecular and Cell  
744 Biology, A-STAR, Singapore) for help in protein sequencing and  
745 critical reading of the manuscript. This work was supported by

National Natural Science Foundation of China grants 746  
N°30470875 and 30771101 to Q.L. 747

### Appendix A. Supplementary data

Supplementary data associated with this article can be found, 750  
in the online version, at doi:10.1016/j.yexcr.2008.02.021. 751

### REFERENCES

- 752
- [1] D. Mazia, Centrosomes and mitotic poles, *Exp. Cell Res.* 753  
153 (1984) 1–15. 755
  - [2] D. Mazia, The chromosome cycle and the centrosome cycle in 756  
the mitotic cycle, *Int. Rev. Cytol.* 100 (1987) 49–92. 757
  - [3] J. Luders, T. Stearns, Microtubule-organizing centres: 758  
a re-evaluation, *Nat. Rev., Mol. Cell Biol.* 8 (2007) 161–167. 759
  - [4] R. Basto, J. Lau, T. Vinogradova, A. Gardiol, C.G. Woods, A. 760  
Khodjakov, J.W. Raff, Flies without centrioles, *Cell* 125 (2006) 761  
1375–1386. 762
  - [5] S. Doxsey, D. McCollum, W. Theaurkauf, Centrosomes in 763  
cellular regulation, *Annu. Rev. Cell Dev. Biol.* 21 (2005) 764  
411–434. 765
  - [6] K. Mikule, B. Delaval, P. Kaldis, A. Jurczyk, P. Hergert, S. 766  
Doxsey, Loss of centrosome integrity induces 767  
p38-p53-p21-dependent G1-arrest, *Nat. Cell Biol.* 9 (2006) 768  
160–170. 769
  - [7] J.S. Andersen, C.J. Wilkinson, T. Mayor, P. Mortensen, E.A. 770  
Nigg, M. Mann, Proteomic characterization of the human 771  
centrosome by protein correlation profiling, *Nature* 426 (2003) 772  
570–574. 773
  - [8] S. Doxsey, W. Zimmerman, K. Mikule, Centrosome control of 774  
the cell cycle, *Trends Cell Biol.* 15 (2005) 303–311. 775
  - [9] M.-F.B. Tsou, T. Stearns, Controlling centrosome number: 776  
licenses and blocks, *Curr. Opin. Cell Biol.* 18 (2006) 74–78. 777
  - [10] G. Sluder, D.A. Begg, Experimental analysis of the reproduction 778  
of spindle poles, *J. Cell Sci.* 76 (1985) 35–51. 779
  - [11] V. Stavropoulou, J.J. Xie, M. Henriksson, B. Tomkinson, S. 780  
Imreh, G.M. Maria, Mitotic infidelity and centrosome 781  
duplication errors in cells overexpressing 782  
tripeptidyl-peptidase II, *Cancer Res.* 65 (2005) 1361–1368. 783
  - [12] G. Sluder, K. Lewis, Relationship between nuclear DNA 784  
synthesis and centrosome reproduction in sea urchin eggs, 785  
*J. Exp. Zool.* 244 (1987) 89–100. 786
  - [13] F. Suizu, A. Ryo, G. Wulf, J. Lim, K.P. Lu, Pin1 regulates 787  
centrosome duplication, and its overexpression induces 788  
centrosome amplification, chromosome instability, and 789  
oncogenesis, *Mol. Cell Biol.* 26 (2006) 1463–1479. 790
  - [14] C.J. Nelsen, R. Kuriyama, B. Hirsch, C. Negron, W.L. Lingle, 791  
M.M. Goggi, M.W. Stanley, J.H. Albrecht, Short-term cyclin D1 792  
overexpression induces centrosome amplification, mitotic 793  
spindle abnormalities, and aneuploidy, *J. Biol. Chem.* 794  
280 (2005) 768–776. 795
  - [15] A. Lindqvist, H. Källström, A. Lundgren, E. Barsoum, C.K. 796  
Rosenthal, Cdc25B cooperates with Cdc25A to induce mitosis, 797  
but has a unique role in activating cyclin B1–Cdk1 at the 798  
centrosome, *J. Cell Biol.* 171 (2005) 35–45. 799
  - [16] A. Duensing, Y. Liu, M. Malumbres, M. Barbacid, S. Duensing, 800  
Cdk2 is dispensable for normal centrosome duplication, but 801  
required for oncogene-induced centrosome overduplication, 802  
*Oncogene* 25 (2006) 2943–2949. 803
  - [17] D.Y. Kim, R. Roy, Cell cycle regulators control centrosome 804  
elimination during oogenesis in *Caenorhabditis elegans*, *J. Cell* 805  
*Biol.* 174 (2006) 751–757. 806
  - [18] P. Tarapore, K. Fukasawa, Loss of p53 and centrosome 807  
hyperamplification, *Oncogene* 21 (2002) 6234–6240. 808

- 809 [19] T. Oikawa, M. Okuda, Z.Y. Ma, R. Goorha, H. Tsujimoto, H.  
810 Inokuma, K. Fukasawa, Transcriptional control of BubR1 by  
811 p53 and suppression of centrosome amplification by BubR1,  
812 Mol. Cell. Biol. 25 (2005) 4046–4061.
- 813 [20] U. Mangold, H. Hayakawa, K. Munger, B.R. Zetter,  
814 Identification of two novel centrosome components  
815 antizyme and antizyme inhibitor and their role in the  
816 regulation of centrosome amplification, Proc. Am. Assoc.  
817 Cancer Res. 47 (2006) 604–605.
- 818 [21] Q. Wang, X.L. Du, J. Meinkoth, Y. Hirohashi, H.T. Zhang, Q.D.  
819 Liu, M. Richter, M.I. Greene, Characterization of Su48, a  
820 centrosome protein essential for cell division, Proc. Natl.  
821 Acad. Sci. U. S. A. 103 (2006) 6512–6517.
- 822 [22] Y. Moroi, C. Peebles, M.J. Fritzler, J. Steigerwald, E.M. Tan,  
823 Autoantibody to centromere (kinetochore) in scleroderma  
824 sera, Proc. Natl. Acad. Sci. U. S. A. 77 (1980) 1627–1631.
- 825 [23] E.M. Tan, Antinuclear antibodies: diagnostic markers for  
826 autoimmune diseases and probes for cell biology, Adv.  
827 Immunol. 44 (1989) 93–151.
- 828 [24] H.J. Ditzel, Human antibodies in cancer and autoimmune  
829 disease, Immunol. Res. 21 (2000) 185–193.
- 830 [25] J.M. Craig, W.C. Earnshaw, P. Vagnarelli, Mammalian  
831 centromeres: DNA sequence, protein composition, and role in  
832 cell cycle progression, Exp. Cell Res. 246 (1999) 249–262.
- 833 [26] D.C. He, C.Q. Zeng, K. Woods, L. Zhong, D. Turner, R.K. Busch,  
834 B.R. Brinkley, H. Busch, CENP-G: a new centromeric protein  
835 that is associated with the alpha-1 satellite DNA subfamily,  
836 Chromosoma 107 (1998) 189–197.
- 837 [27] J.H. Shero, B.L. Bordwel, N.F. Rothfield, W.C. Earnshaw, High  
838 titers of autoantibodies to topoisomerase I (Scd-70) in sera  
839 from scleroderma patients, Science 231 (1986) 737–740.
- 840 [28] R.J. Kipnis, J. Craft, J.A. Hardin, The analysis of antinuclear and  
841 antinucleolar autoantibodies of scleroderma by  
842 radioimmunoprecipitation assays, Arthritis Rheum. 33 (1990)  
843 1431–1437.
- 844 [29] M.R. Lerner, J.A. Steitz, Antibodies to small nuclear RNAs  
845 complexed with proteins are produced by patients with  
846 systemic lupus erythematosus, Proc. Natl. Acad. Sci. U. S. A.  
847 76 (1979) 5495–5499.
- 848 [30] R.S. Johnson, J.A. Taylor, Sequence database searches via *de*  
849 *nov* peptide sequencing by tandem mass spectrometry,  
850 Mol. Biotechnol. 22 (2002) 301–315.
- 851 [31] V. Dancik, T.A. Addona, K.R. Clauser, J.E. Vath, P.A. Pevzner,  
852 *De novo* peptide sequencing via tandem mass spectrometry:  
853 a graph-theoretical approach, J. Comput. Biol. 6 (1999)  
854 327–342.
- 855 [32] T. Chen, M.Y. Kao, M. Tepel, J. Rush, G.M. Church, A dynamic  
856 programming approach for *de novo* peptide sequencing via  
857 tandem mass spectrometry, J. Comput. Biol. 8 (2001) 325–337.
- 858 [33] B. Lu, T. Chen, A suboptimal algorithm for *de novo* peptide  
859 sequencing via tandem mass spectrometry, J. Comput. Biol.  
860 10 (2003) 1–12.
- 861 [34] J. Kanski, A. Behring, Proteomic identification of  
862 3-nitrotyrosine-containing rat cardiac proteins: effects of  
863 biological aging, Am. J. Physiol. Heart C. 288 (2005) H371–H381.
- 864 [35] G. Tezel, X.J. Yang, J. Cai, Proteomic identification of  
865 oxidatively modified retinal proteins in a chronic  
866 pressure-induced rat model of glaucoma, Invest. Ophth. Vis.  
867 Sci. 46 (2005) 177–3187.
- 868 [36] M. Luo, S. Reyna, L. Wang, Z. Yi, C. Carroll, L.Q. Dong, P.  
869 Langlais, S.T. Weintraub, L.J. Mandarino, Identification of  
870 insulin receptor substrate 1 serine/threonine  
871 phosphorylation sites using mass spectrometry analysis:  
872 regulatory role of serine 1223, Endocrinology 146 (2005)  
873 4410–4416.
- 874 [37] M.R. Wilkins, I. Lindskog, E. Gasteiger, A. Bairoch, J.C. Sanchez,  
875 D.F. Hochstrasser, R.D. Appel, Detailed peptide characterization  
876 using PEPTIDEMASS—a World-Wide-Web-accessible tool,  
877 Electrophoresis 18 (1997) 403–408.
- [38] J. Schultz, F. Milpetz, P. Bork, C.P. Ponting, SMART, a simple 878  
modular architecture research tool: identification of signaling 879  
domains, Proc. Natl. Acad. Sci. U. S. A. 95 (1998) 5857–5864. 880
- [39] I. Letunic, L. Goodstadt, N.J. Dickens, T. Doerks, J. Schultz, R. 881  
Mott, F. Ciccarelli, R.R. Copley, C.P. Ponting, P. Bork, Recent 882  
improvements to the SMART domain-based sequence 883  
annotation resource, Nucleic Acids Res. 30 (2002) 242–244. 884
- [40] Y.P. Ching, S.F. Chan, K.T. Jeang, D.Y. Jin, The retroviral 885  
oncoprotein Tax targets the coiled-coil centrosomal protein 886  
TAX1BP2 to induce centrosome overduplication, Nat. Cell 887  
Biol. 8 (2006) 717–724. 888
- [41] L. Falquet, M. Pagni, P. Bucher, N. Hulo, C.J. Sigrist, K. 889  
Hofmann, A. Bairoch, The PROSITE database, its status in 890  
2002, Nucleic Acids Res. 30 (2002) 235–238. 891
- [42] S. Toji, N. Yabuta, T. Hosomi, S. Nishihara, T. Kobayashi, S. 892  
Suzuki, K. Tamai, H. Nojima, The centrosomal protein Lats2 is 893  
a phosphorylation target of Aurora-A kinase, Genes Cells 894  
9 (2004) 383–397. 895
- [43] H. Shin, H. Kobayashi, M. Kitamura, S. Waguri, T. Suganuma, 896  
Y. Uchiyama, K. Nakayama, Roles of ARFRP1 897  
(ADP-ribosylation factor-related protein 1) in post-Golgi 898  
membrane trafficking, J. Cell Sci. 118 (2005) 4039–4048. 899
- [44] L. Lu, W.J. Hong, Interaction of Arl1-GTP with GRIP domains 900  
recruits autoantigens Golgin-97 and Golgin-245/p230 onto the 901  
Golgi, Mol. Biol. Cell 14 (2003) 3767–3781. 902
- [45] L. Lu, G. Tai, M. Wu, H. Song, W. Hong, Multilayer interactions 903  
determine the Golgi localization of GRIP golgins, Traffic 904  
7 (2006) 1399–1407. 905
- [46] E.U. Saelman, P.J. Keely, S.A. Santoro, Loss of MDCK cell alpha 906  
2 beta 1 integrin expression results in reduced cyst formation, 907  
failure of hepatocyte growth factor/scatter factor-induced 908  
branching morphogenesis, and increased apoptosis, J. Cell 909  
Sci. 108 (1995) 3531–3540. 910
- [47] V.B. Castaing, M. Moudjou, D.J.P. Ferguson, S. Mucklow, Y. 911  
Belkaid, G. Milon, P.R. Crocker, Molecular characterisation of 912  
ninein, a new coiled-coil protein of the centrosome, J. Cell Sci. 913  
109 (1996) 179–190. 914
- [48] J. Yang, X.Q. Liu, G.H. Yue, M. Adamian, O. Bulgakov, T. Li, 915  
Rootletin, a novel coiled-coil protein, is a structural 916  
component of the ciliary rootlet, J. Cell Biol. 159 (2002) 917  
431–440. 918
- [49] T. Ohta, R. Essner, J.H. Ryu, R.E. Palazzo, Y. Uetake, R. 919  
Kuriyama, Characterization of Cep135, a novel coiled-coil 920  
centrosomal protein involved in microtubule organization in 921  
mammalian cells, J. Cell Biol. 156 (2002) 87–99. 922
- [50] L. Romio, A.M. Fry, P.J.D. Winyard, S. Malcolm, A.S. Woolf, S.A. 923  
Feather, OFD1 is a centrosomal/basal body protein expressed 924  
during mesenchymal-epithelial transition in human 925  
nephrogenesis, J. Am. Soc. Nephrol. 15 (2004) 2556–2568. 926
- [51] M. Takahashi, A. Yamagiwa, T. Nishimura, H. Mukai, Y. Ono, 927  
Centrosomal proteins CG-NAP and kendrin provide 928  
microtubule nucleation sites by anchoring g-tubulin ring 929  
complex, Mol. Biol. Cell 13 (2002) 3235–3245. 930
- [52] J.B. Dichtenberg, W. Zimmerman, C.A. Sparks, A. Young, C. 931  
Vidair, Y. Zheng, W. Carrington, F.S. Fay, S.J. Doxsey, 932  
Pericentrin and  $\gamma$ -tubulin form a protein complex and are 933  
organized into a novel lattice at the centrosome, J. Cell Biol. 934  
141 (1998) 163–174. 935
- [53] M.J. Fritzler, C.C. Lung, J.C. Hamel, K.J. Griffith, E.K. Chan, 936  
Molecular characterization of Golgin-245, a novel Golgi 937  
complex protein containing a granin signature, J. Biol. Chem. 938  
270 (1995) 31262–31268. 939
- [54] C. Infante, F. Ramos-Morales, C. Fedriani, M. Bornens, R.M. 940  
Rios, GMAP-210, a cis-Golgi network-associated protein, is a 941  
minus end microtubule-binding protein, J. Cell Biol. 145 (1999) 942  
83–98. 943
- [55] T. Mikiko, S. Hideki, S. Masaki, M. Masaaki, M. Hideyuki, O. 944  
Yoshitaka, Characterization of a novel giant scaffolding 945  
protein, CG-NAP, that anchors multiple signaling enzymes to 946

- 947 centrosome and the Golgi apparatus, *J. Biol. Chem.* 274 (1999) 984  
 948 17267–17274. 985
- 949 [56] R.C. Eisman, N. Stewart, D. Miller, T.C. Kaufman, Centrosomin's 986  
 950 beautiful sister (cbs) encodes a GRIP-domain protein that marks 987  
 951 Golgi inheritance and functions in the centrosome cycle in 988  
 952 *Drosophila*, *J. Cell Sci.* 119 (2006) 3399–3412. 989
- 953 [57] R.A. Shanks, B.T. Steadman, P.H. Schmidt, J.R. Goldenring, 990  
 954 AKAP350 at the Golgi apparatus, *J. Biol. Chem.* 277 (2002) 991  
 955 40967–40972. 992
- 956 [58] H.A. Fisk, C.P. Mattison, M. Winey, Centrosome and tumor 993  
 957 suppressors, *Curr. Opin. Cell Biol.* 14 (2002) 700–705. 994
- 958 [59] B. Short, A. Haas, F.A. Barr, Golgins and GTPases, giving 995  
 959 identity and structure to the Golgi apparatus, *Biochim.* 996  
 960 *Biophys. Acta* 1744 (2005) 383–395. 997
- 961 [60] F.A. Barr, H.W. Sillje, E.A. Nigg, Polo-like kinases and the 998  
 962 orchestration of cell division, *Nat. Rev., Mol. Cell Biol.* 5 (2004) 999  
 963 429–440. 1000
- 964 [61] M. Casenghi, F.A. Barr, E.A. Nigg, Phosphorylation of Nlp by 1001  
 965 Plk1 negatively regulates its dynein-dynactin-dependent 1002  
 966 targeting to the centrosome, *J. Cell Sci.* 118 (2005) 5101–5108. 1003
- 967 [62] A. Kramer, N. Mailand, C. Lukas, R.G. Syljuasen, C.J. 1004  
 968 Wilkinson, E.A. Nigg, J. Bartek, J. Lukas, 1005  
 969 Centrosome-associated Chk1 prevents premature activation 1006  
 970 of cyclin-B-Cdk1 kinase, *Nat. Cell Biol.* 6 (2004) 884–891. 1007
- 971 [63] B.M. Lange, Integration of the centrosome in cell cycle control, 1008  
 972 stress response and signal transduction pathways, 1009  
 973 *Curr. Opin. Cell Biol.* 14 (2002) 35–43. 1010
- 974 [64] M. Okuda, H.F. Horn, P. Tarapore, Y. Tokuyama, A.G. Smulian, 1011  
 975 P.K. Chan, E.S. Knudsen, I.A. Hofmann, J.D. Snyder, K.E. Bove, 1012  
 976 K. Fukasawa, Nucleophosmin/B23 is a target of CDK2/cyclin E 1013  
 977 in centrosome duplication, *Cell* 103 (2000) 127–140. 1014
- 978 [65] M.P. Shekhar, A. Lyakhovich, D.W. Visscher, H. Heng, N. 1015  
 979 Kondrat, Rad6 overexpression induces multinucleation, 1016  
 980 centrosome amplification, abnormal mitosis, aneuploidy, 1017  
 981 and transformation, *Cancer Res.* 67 (2002) 2115–2124. 1018
- 982 [66] E.H. Hinchcliffe, C. Li, E.A. Thompson, J.L. Maller, G. Sluder, 1019  
 983 Requirement of cdk2-cyclin E activity for repeated 1020  
 centrosome reproduction in *Xenopus* egg extracts, *Science* 984  
 283 (1999) 851–854. 985
- [67] K. Kawamura, H. Izumi, Z.Y. Ma, R. Ikeda, M. Moriyama, T. 986  
 Tanaka, T. Nojima, L.S. Levin, K. Fujikawa-Yamamoto, K. 987  
 Suzuki, K. Fukasawa, Induction of centrosome amplification 988  
 and chromosome instability in human bladder cancer cells by 989  
 p53 mutation and cyclin E overexpression, *Cancer Res.* 990  
 64 (2004) 4800–4809. 991
- [68] W. Lutz, W.L. Lingle, D. McCormick, T.M. Greenwood, J.L. 992  
 Salisbury, Phosphorylation of centrin during the cell cycle and 993  
 its role in centriole separation preceding centrosome 994  
 duplication, *J. Biol. Chem.* 276 (2001) 20774–20780. 995
- [69] Y. Tokuyama, H.F. Horn, K. Kawamura, P. Tarapore, K. 996  
 Fukasawa, Specific phosphorylation of nucleophosmin on 997  
 Thr<sup>199</sup> by cyclin-dependent kinase 2-cyclin E and its role in 998  
 centrosome duplication, *J. Biol. Chem.* 276 (2001) 21529–21537. 999
- [70] S.J. Vidwans, M.L. Wong, P.H. O, Farrell, Mitotic regulators 1000  
 govern progress through steps in the centrosome duplication 1001  
 cycle, *J. Cell Biol.* 147 (1999) 1371–1377. 1002
- [71] L.H. Yih, Y.Y. Tseng, Y.C. Wu, T.C. Lee, Induction of 1003  
 centrosome amplification during arsenite-induced mitotic 1004  
 arrest in CGL-2 cells, *Cancer Res.* 66 (2006) 2098–2106. 1005
- [72] H. Muller, M.L. Fogeron, V. Lehmann, H. Lehrach, B.M. Lange, 1006  
 A centrosome-independent role for gamma-TuRC 1007  
 proteins in the spindle assembly checkpoint, *Science* 1008  
 314 (2006) 654–657. 1009
- [73] K. Fukasawa, T. Choi, R. Kuriyama, S. Rulong, G.F. 1010  
 Vande-Woude, Abnormal centrosome amplification in the 1011  
 absence of p53, *Science* 271 (1996) 1744–1747. 1012
- [74] Q.J. Liang, D.C. He, Y.C. Wang, An analysis of the gene 1013  
 expression of a centromere constitutive protein CenpG 1014  
 affected by antisense CenpB, *High Technol. Lett.* 11 (2005) 1015  
 217–220. 1016
- [75] R.M. Guzzo, S. Sevinc, M. Saliy, B.S. Tuana, A novel isoforms of 1017  
 sarcolemmal membrane-associated protein (SLMAP) is a 1018  
 component of the microtubule organizing centre, *J. Cell Sci.* 1019  
 117 (2004) 2271–2281. 1020